ELSEVIER

Comparative Biochemistry and Physiology Part A 133 (2002) 967–978

CBP

www.elsevier.com/locate/cbpa

Morphology and mechanics of myosepta in a swimming salamander (*Siren lacertina*)☆

Emanuel Azizi[a,*], Gary B. Gillis[b,1], Elizabeth L. Brainerd[a]

[a]*Organismic and Evolutionary Biology Program and Biology Department, University of Massachusetts, 611 North Pleasant Street, Amherst, MA 01003-9297, USA*

[b]*Department of Organismic and Evolutionary Biology, Concord Field Station, Harvard University, Bedford, MA, USA*

Received 9 January 2002; received in revised form 8 July 2002; accepted 22 July 2002

Abstract

In contrast to the complex, three-dimensional shape of myomeres in teleost fishes, the lateral hypaxial muscles of salamanders are nearly planar and their myosepta run in a roughly straight line from mid-lateral to mid-ventral. We used this relatively simple system as the basis for a mathematical model of segmented musculature. Model results highlight the importance of the mechanics of myosepta in determining the shortening characteristics of a muscle segment. We used sonomicrometry to measure the longitudinal deformation of myomeres and the dorsoventral deformation of myosepta in a swimming salamander (*Siren lacertina*). Sonomicrometry results show that the myosepta allow some dorsoventral lengthening, indicating an amplification of myomere shortening that is greater than that produced by muscle fiber angle alone (10% muscle fiber shortening produces 28.7% myomere shortening). Polarized light and DIC microscopy of isolated hypaxial myosepta revealed that the collagen fiber orientation in hypaxial myomeres is primarily mediolateral. The mediolateral collagen fiber orientation, combined with our finding that the hypaxial myosepta lengthen dorsoventrally during swimming, suggests that one possible function of hypaxial myosepta in *S. lacertina* is to increase the strain amplification of the muscle fibers by reducing the mediolateral bulging of the myomeres and redirecting the bulging toward the dorsoventral direction.

Keywords: Caudata; Biomechanics; Myosepta; Myomere; Segmented muscle; Muscle architecture; Urodela; Sonomicrometry

1. Introduction

The presence of axial muscle segmentation is an important aspect of the primitive body plan and locomotory habits of vertebrates (Gans, 1989). The axial musculature of fishes and some amphibians retains the defining characteristics of this body plan, including the presence of segmented muscle blocks (myomeres) that attach to connective tissue sheets (myosepta). In teleost fishes, these myomeres and myosepta are folded into nested cones, each of which spans several vertebral segments (Greene and Greene, 1913; Maurer, 1913; Shann, 1914). Numerous studies have focused on the function of this complex axial musculature in undulatory locomotion (e.g. Willemse, 1966; Alexander, 1969; Wainwright, 1983; Rome et al.

☆ This paper was presented at 'Tendon – Bridging the Gap', a symposium at the 2002 Society of Integrative and Comparative Biology. Participation was funded by the SICB, The Shriners Hospitals for Children, and the National Science Foundation (IBN-0127260).

*Corresponding author. Tel.: +1-413-545-1863; fax: +1-413-545-3243.

E-mail address: mannya@bio.umass.edu (E. Azizi).

[1] Present address: Department of Biology, Mt. Holyoke College, South Hadley MA, USA.

1095-6433/02/$ - see front matter © 2002 Elsevier Science Inc. All rights reserved.
PII: S1095-6433(02)00223-4

1993; Jayne and Lauder, 1995; Westneat et al., 1998; Shadwick et al., 1999; Wakeling and Johnston, 1999), but a clear understanding of the relationship between overall body bending and muscle fiber trajectory, myomere shape and the mechanics of myosepta and other axial connective tissues has remained elusive.

In contrast to the complex, three-dimensional shape of myomeres in teleost fishes, the lateral hypaxial muscles of salamanders are nearly planar and their myosepta run in a roughly straight line from mid-lateral to ventral (Fig. 1; Maurer, 1911; Simons and Brainerd, 1999; Brainerd and Simons, 2000). Based on the relatively simple lateral hypaxial muscles of salamanders, a generalized mathematical model of segmented muscle architecture has been developed (Brainerd and Azizi, unpublished). The goal of this model is to relate the amount of longitudinal segment shortening to initial muscle fiber angle and the dorsoventral deformation of myosepta.

The model simplifies a hypaxial myomere of a salamander to a rectangular box of constant volume with initial segment length (S_o), height (H_o), and depth (D_o), and with a single muscle fiber (L), which attaches to each side of the box (myosepta) at an initial angle α (Fig. 2). As the muscle fiber shortens from L to fL, the dimensions of the segment change to S, H and D and the muscle fiber angle changes from α to β. We assume that in order to produce lateral bending, the segment always shortens in the longitudinal (S) direction during muscle fiber shortening. We vary the constraints set on the deformation of segment height (H) and constrain the mediolateral depth (D) of the segment to increase (although by different amounts based on constraints set on H) in order to maintain the constant volume of the muscle block.

Results from the mathematical model indicate that, for a given percentage of muscle fiber shortening (muscle fiber strain), the percentage of longitudinal segment shortening (segment strain) depends strongly on whether the dorsoventral height (H) of the myomere decreases (Fig. 2a), remains constant (Fig. 2b), or increases (Fig. 2c). If we assume that the height of the myomere decreases in response to the vertical component of angled muscle fiber shortening (Fig. 2a), then H and S shorten in equal proportions and the segment bulges mediolaterally (D) to maintain a constant volume. In this shortening condition, segment strain equals muscle fiber strain and the results are independent of muscle fiber angle. If we assume that H remains constant and D again increases to maintain constant volume (Fig. 2b), then segment strain is greater than muscle fiber strain (for initial muscle fiber angles $\alpha > 0$). If we assume that H increases (Fig. 2c), then muscle fiber shortening is amplified even more than if H is held constant. Fig. 2c shows a condition in which H and D increase in equal proportions to maintain a constant segment volume (Alexander, 1969). The generalized model describes a continuum of possible changes in H and D; we have selected the three shown in Fig. 2 to demonstrate the effect of changes in H on segment strain amplification.

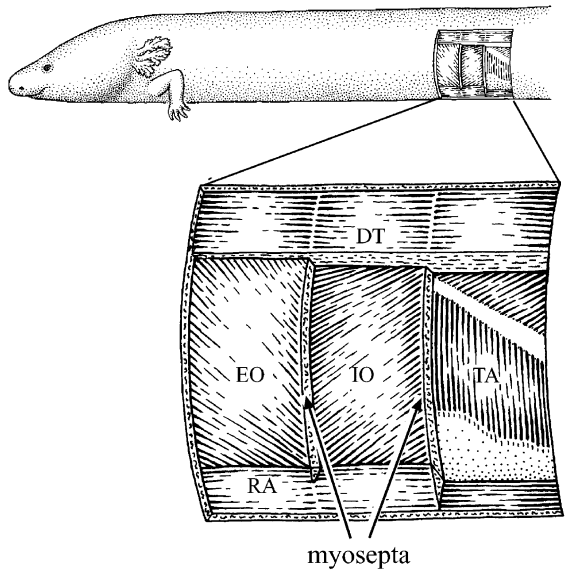

Fig. 1. Lateral view of the axial musculature of *Siren lacertina*. In the three myomeres shown, hypaxial muscle layers are exposed from superficial to deep in the cranial to caudal direction. In the hypaxial region, the myosepta are oriented mediolaterally and span from the peritoneum (medially) to the skin (laterally). *Abbreviations:* DT, dorsalis trunci; EO, external oblique; IO, internal oblique; RA, rectus abdominis; TA, transverse abdominis (modified from Simons and Brainerd, 1999).

Strain amplification occurs only when initial muscle fiber angle is greater than zero ($\alpha > 0$). This result indicates that in segments with longitudinally oriented muscle fibers ($\alpha = 0$), such as the lateral red muscle of fishes, segment strain is not amplified. However, when H is constant or increases, strain amplification increases with increasing muscle fiber angle when initial muscle fiber angle $\alpha > 0$.

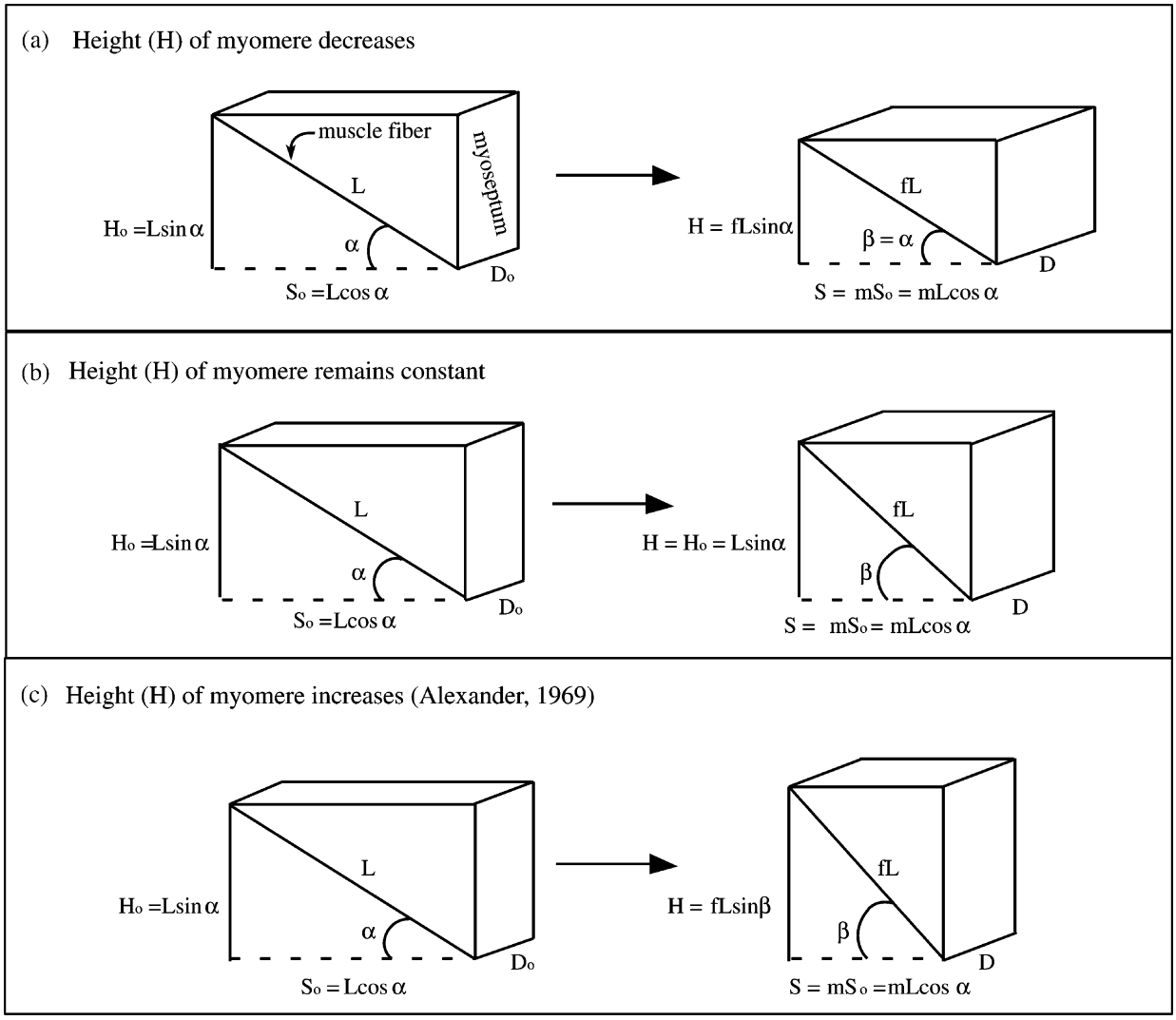

Fig. 2. A mathematical model of segmented musculature with three conditions of myomere deformation. Figures are drawn to scale and in all three conditions, the muscle fiber (*L*) is shown to shorten by 20%, to a final length fraction (*f*) of 0.8. (a) Dorsoventral height (*H*) and longitudinal length (*S*) of the segment decrease by equal percentages as the muscle fiber shortens from *L* to *fL*. (b) *H* remains constant as the muscle fiber shortens. (c) *H* increases as the muscle fiber shortens. These three conditions represent three points along a continuum of possible myomere deformations. Note that myomere shortening is greatest when the myomere lengthens dorsoventrally. Definition of variables: α and β, muscle fiber angle before and after muscle contraction; S_o and *S*, length of myomere before and after muscle contraction; H_o and *H*, height of myosepta before and after contraction; D_o and *D*, depth of segment before and after muscle contraction; *L*, initial muscle fiber length; *f*, final muscle fiber length fraction; m, final myomere length fraction.

The effects of this strain amplification can be seen most clearly if we place a series of myomeres together, and look at the effects of the three myomere deformation conditions on overall body bending (Fig. 3). If the myomeres shorten dorsoventrally during segment shortening (*H* decreases), then segment shortening is not amplified and 10% muscle fiber shortening produces 10% shortening of the lateral edge of the body (Fig. 3b) irrespective of initial muscle fiber angle. If the dorsoventral height of the myomeres remains constant (Fig. 3c), segment shortening is amplified and 10% muscle fiber shortening produces 15.3% longitudinal shortening of the lateral edge of the body (calculated here for an initial muscle fiber angle $\alpha = 35°$). If the myomeres lengthen dorsoventrally (Fig. 3d), then 10% muscle fiber shortening produces 26.5% shortening of the lateral edge of the

body (initial muscle fiber angle $\alpha = 35°$). These results highlight the potential importance of the myosepta in determining the shortening characteristics of the myomeres. If the collagen fiber orientation of the myosepta allows the dorsoventral height of the myomeres to increase, then strain amplification can be maximized (Fig. 2c and Fig. 3d).

This model is similar to a model proposed by Alexander (1969), but the new model includes the possibility that the material properties of myosepta or other connective tissues may influence the changes in height and depth of the segment during longitudinal shortening. The model by Alexander (1969) assumes that longitudinal shortening is offset by equal amounts of bulging in height and depth, as would be the case for an isolated block of muscle tissue (Alexander's model is identical to the shortening condition shown in Fig. 2c). In the new model, myomeres are allowed to bulge differentially in height and depth, within the constraint that muscle volume must be conserved. This model allows us to explore the interaction between muscle fiber angle and the effects of axial connective tissues on the bulging of myomeres during contraction.

We have selected the abdominal myomeres of an elongate salamander (*Siren lacertina*) to test the mathematical model because a number of the simplifying assumptions made in our model are appropriate for this system. The shape of hypaxial myomeres from the abdominal region of *S. lacertina* is nearly planar and closely resembles the shape of the model. In our model we assume that the adjacent myosepta do not translate differentially (shear) in the vertical direction due to long axis torsion. This assumption is reasonable given that the lateral hypaxial musculature of *S. lacertina* has two layers (EO and IO) with opposing muscle fiber angles (Fig. 1). These layers have been shown to be active simultaneously during swimming (Carrier, 1993; Bennett et al., 2001) and have been hypothesized to function in resisting long axis torsion. In addition, the abdominal region of *S. lacertina*, which makes up 60% of total body length, undergoes significant lateral undulation during steady swimming, a necessary condition for testing our segment shortening model (Gillis, 1997).

In the present study, we describe the gross morphology and collagen fiber orientation of myosepta from the abdominal region of *S. lacertina*. We also use sonomicrometry to measure the dynamics of hypaxial myosepta during swimming. We use these empirical data in a mathematical

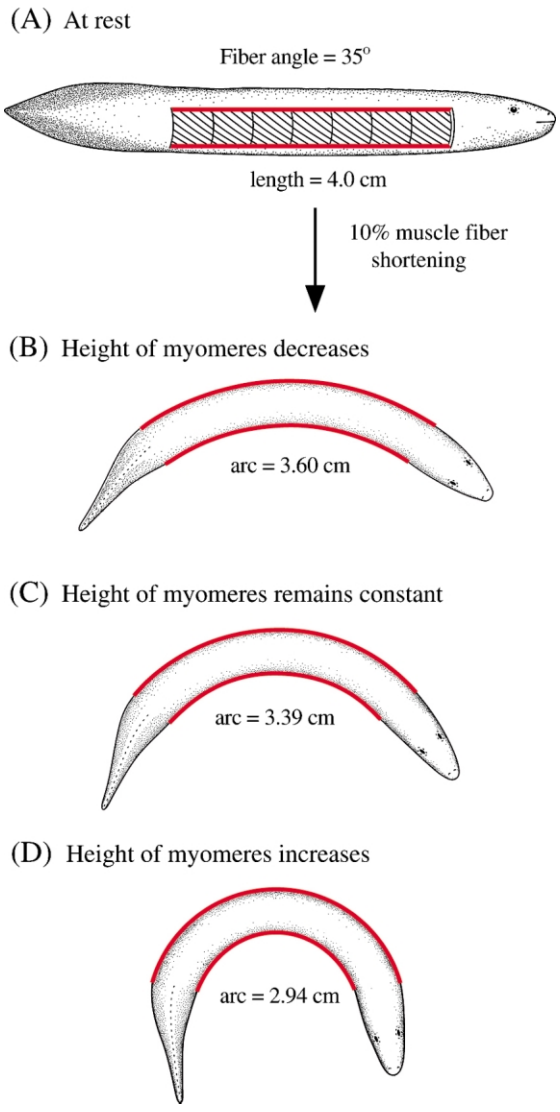

Fig. 3. Effect of three modes of myomere deformation on axial bending during 10% muscle fiber shortening (drawings are to scale). (A) Generalized elongate vertebrate shown at rest, with an initial muscle fiber angle of 35° and a trunk length (shown in red) of 4 cm. Predicted values of myomere shortening were used to calculate a radius of curvature for a beam with a length of 4 cm and a diameter of 0.6 cm. (B) If the myomeres decrease in height, then 10% muscle fiber shortening leads to 10% shortening of the right side of the body (from 4 to 3.6 cm). (C) If myomere height remains constant, then 10% fiber shortening leads to 15.3% shortening of the right side of the body (from 4 to 3.39 cm). (D) If myomere height increases, then 10% muscle fiber shortening leads to 26.5% shortening of the right side of the body (from 4 to 2.94 cm).

model of segmented musculature to predict strain amplification in the lateral hypaxial musculature of *S. lacertina*. Our goal in this study is to combine mathematical modeling, descriptive morphology, and in vivo sonomicrometry measurements to develop a more rigorous understanding of the function of myosepta.

2. Materials and methods

2.1. Morphology

We examined the morphology of myosepta in two adult and two juvenile specimens of *Siren lacertina* (Le Conte) obtained from the University of Massachusetts Museum of Natural History. The two adult specimens had total lengths of 53 cm (SVL = 38.5 cm) and 55 cm (SVL = 40 cm) and the juveniles had total lengths of 15 cm (SVL = 10 cm) and 19 cm (SVL = 13 cm). All the specimens used in this study were fixed in 10% buffered formalin. The three-dimensional shape and spatial arrangement of myosepta were determined through a combination of gross dissection of the adult specimens and clearing and staining of the juvenile specimens.

The juvenile specimens were skinned, cleared and double stained and then transferred stepwise to 100% alcohol to allow for easier visualization of the myosepta (Gemballa and Britz, 1998). To examine the orientation of collagen fibers within the myosepta, individual myosepta were dissected from the caudal part of the abdominal region at longitudinal positions ranging from 0.55 to 0.70 TL. Some of the extracted myosepta included both the hypaxial and epaxial regions, but most of the dissections were limited to the hypaxial region. Using a trypsin solution (10 g l^{-1}), the extraneous musculature attached to the myosepta was removed. Once nearly all of the attached musculature was enzymatically digested, the myosepta were transferred to a solution of 70% ethanol. Polarized light microscopy and low magnification differential interference contrast (DIC) microscopy were used to visualize the orientation of collagen fibers within the myosepta. Due to the different refractive properties of collagen and the surrounding matrix, collagen fibers can be easily observed using both polarized light and DIC microscopy (Gemballa and Britz, 1998). Myosepta were photographed using a SPOT camera mounted on a Nikon E600 compound microscope.

2.2. Sonomicrometry

Sonomicrometry has become a valuable tool for measuring muscle deformation in vivo (e.g. Shadwick et al., 1999; Gillis and Biewener, 2000). This technique utilizes piezoelectric crystals that sequentially send and receive ultrasonic signals. The time between the transmission of a signal by one crystal and the reception of that signal by another crystal is converted to a distance using the speed of sound in muscle (1.54×10^3 m/s). In this study, we used the Sonometrics Digital Ultrasonic Measurement System (TRX series 6) to measure the longitudinal deformation of the myomeres and the dorsoventral deformation of the myosepta.

Two adult *Siren lacertina* (TL = 57 cm; SVL = 41 cm) and (TL = 49.5 cm; SVL = 34 cm) were purchased from a commercial herpetological vendor and used in three separate sonomicrometry experiments. The salamanders were housed in glass aquaria partially filled with water and sphagnum moss and maintained at room temperature (22 °C). The salamanders were normally kept on a diet of four earthworms per week but were not fed for 3 days prior to the sonomicrometry experiments. All animal care and experimental protocols were approved by the University of Massachusetts Amherst Institutional Animal Care and Use Committee.

In two experiments we measured the longitudinal deformation of the myomeres and the dorsoventral deformation of the myosepta during steady swimming (in the third experiment similar measurements were made during startle responses; see below). Sonomicrometry crystals were implanted in the caudal part of the abdominal region at the 27th myomere (0.68 TL, 0.71TL). This longitudinal position was selected as the surgical site because the hypaxial myomeres and myosepta in this region are roughly planar, and substantial lateral displacement occurs in this region during steady swimming (Gillis, 1997). The salamanders were anesthetized using a buffered solution of 1 g l^{-1} tricaine methanesulfonate (MS 222) and four sonomicrometry crystals (1 mm in diameter) were surgically implanted subcutaneously. In order to minimize the surgical trauma to the 27th myomere, we used small incisions (approx. 5 mm) in the 26th and 28th myomere to gain access to the myosepta of the external oblique muscle layer (Fig. 1). The tips of the crystals were then pushed through a small incision (1 mm) in the myosepta,

and the leads were sutured tightly to both the myosepta and the skin (the crystals themselves were embedded in the external oblique musculature). The four crystals were configured into a rectangle, with one pair of crystals directly attached to the 27th myoseptum and another pair directly attached to the 28th myoseptum. This configuration allowed for two independent length measurements of both the myosepta (dorsoventral deformation) and the myomere (longitudinal deformation) during locomotion. The salamanders were given approximately an hour to recover from the anesthetic, placed in a 250×60×30 cm water-filled trackway and filmed in dorsal view (miniDV format, 30 frames per s).

To correlate the sonomicrometry data with steady swimming kinematics, the sonomicrometry traces were superimposed onto the video sequences using a TelevEyes/Pro video overlay box (Digital Vision Inc.). In one experiment, data were collected at 125 Hz with a transmit pulse of 110 ns and an inhibit delay of 2.3 mm (SonoLab 3.1.4). In the second experiment, data were collected at 100 Hz with a transmit pulse of 110 ns, and an inhibit delay of 4.2 mm. The data were converted to ASCII files and exported to SonoView 3.1.4 for post-processing. We limited our analysis to sequences of steady swimming that included a minimum of four complete tailbeat cycles. Each sequence was removed of outliers and smoothed using a running average algorithm. In the first experiment, data from 25 swimming sequences were analyzed using a reduced major axis (RMA) regression to determine the relationship between the dorsoventral lengths of the myosepta and the longitudinal length of the myomere. In the second experiment, 15 swimming sequences were similarly analyzed using a RMA regression. This regression model was used because it assumes equal error associated with the sonomicrometry measurements in both the dorsoventral and longitudinal directions.

In a third experiment, we measured the longitudinal deformation of the myomeres and the dorsoventral deformation of the myosepta during the high amplitude body bending associated with startle responses in *S. lacertina*. Sonomicrometry crystals were implanted in the middle of the abdominal region at the 16th myomere (0.51 TL). This body position is characterized by substantial axial bending during startle responses and was, therefore, an ideal site for this sonomicrometry experiment. Using similar surgical procedures to those described above, four crystals were configured into a cross. Three longitudinally oriented crystals were placed on the dorsal regions of the 15th, 16th and 17th hypaxial myosepta with a fourth crystal placed ventrally on the 16th myoseptum. The salamander was given approximately 2 h to recover from the anesthetic, placed in a 60×60×30 cm tank and filmed in dorsal view. To produce axial bending, we induced a startle response in the salamander, and collected data at 250 Hz with a transmit pulse of 125 ns, and an inhibit delay of 2.3 mm (SonoLab 3.1.4). The data were converted to ASCII files and exported to SonoView 3.1.4 for post-processing. For the 10 escape sequences analyzed, the relationship between the dorsoventral length of the myosepta and the longitudinal length of the myomere were determined using a RMA regression. All statistical tests were performed using JMP version 4.0 (SAS Inc.).

3. Results

3.1. Morphology

In the abdominal region, the hypaxial myosepta in *Siren lacertina* have a roughly planar geometry and are oriented perpendicular to the long axis of the body (Fig. 1). The myosepta attach to the skin laterally and to the peritoneum medially (Fig. 4a). The attachment of each myoseptum to the skin forms an external costal groove. At the ventral midline, myosepta are oriented anteromedially and begin to converge, creating the ventral portion of the vertical septum.

Based on polarized light and DIC microscopy, we determined that the collagen fibers within the hypaxial region of abdominal myosepta are oriented primarily mediolaterally (Figs. 4 and 5). However, in the most ventral region of the myosepta, the collagen fiber orientation shifts from mediolateral to approximately dorsoventral (i.e. the fibers are radially arranged around the abdominal cavity). In the epaxial myosepta, the collagen fibers are primarily oriented longitudinally. The observed fiber architecture was largely consistent between all individuals examined.

Although no distinct horizontal septum was observed, the myosepta extend anteromedially at the boundary of the hypaxial and epaxial regions (Fig. 5). This anteromedial extension connects

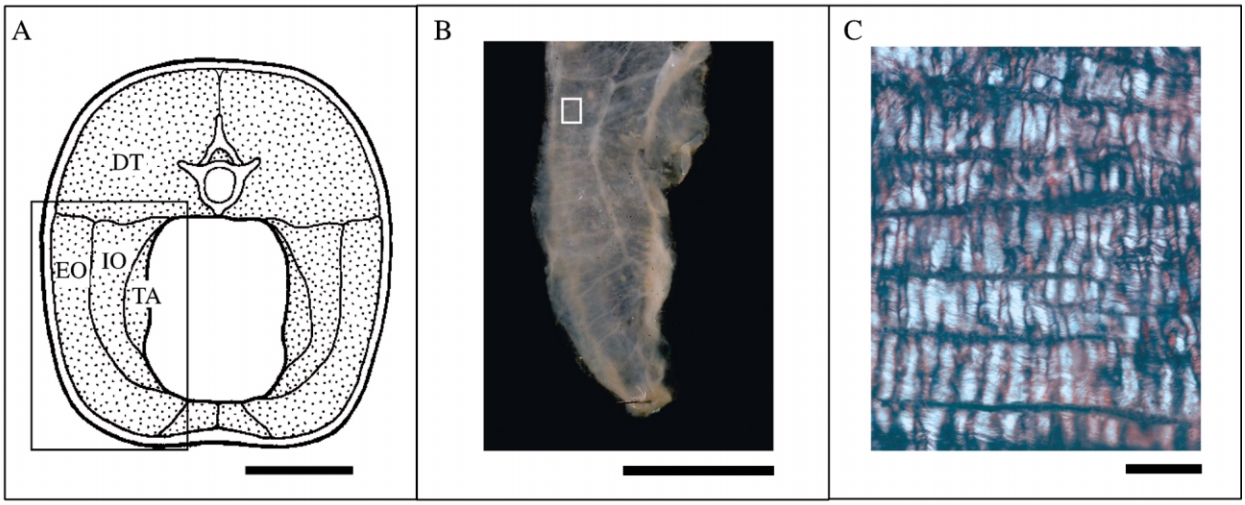

Fig. 4. Collagen fiber orientation within hypaxial myosepta. (A) Transverse section of *Siren lacertina* highlighting the hypaxial region of the myomeres. The medial edges of myosepta attach to the peritoneum and the lateral edges to the skin. *Abbreviations:* DT, dorsalis trunci; EO, external oblique; IO internal oblique; TA transverse abdominis. Scale bar = 1 cm. (B) Anterior view of the hypaxial region of a single myoseptum isolated using dissection and muscle digestion. White box indicates area magnified in next panel. Scale bar = 1 cm. (C) Magnified view of a hypaxial myoseptum viewed under polarized light. Collagen fibers are oriented horizontally and crimps in the fibers appear as vertical bands. Scale bar = 40 μm.

each individual myoseptum to the dorsal surface of the peritoneum and to the transverse process of the next anterior vertebra. Similar to the myosepta of *Ambystoma mexicanum* (Ebmeyer and Gemballa, 2001), the epaxial region of each myoseptum consists of a broad anteromedially oriented section, which connects two small myoseptal cones. A dorsal posterior cone (DPC) is located lateral to the neural spines and a secondary anterior cone (SAC) is located at the anterior edge of the myosepta near the dorsal midline (Fig. 5). The medial portion of the SAC extends caudally and converges with posterior myosepta. The epaxial myosepta span two full vertebral segments. At the dorsal midline, adjacent myosepta from both sides of the body converge, creating the appearance of a vertical septum. While the abdominal myosepta are dorsoventrally asymmetrical, this asymmetry decreases in the caudal region.

3.2. Sonomicrometry

We present the results from three sonomicrometry experiments on two individual *Siren lacertina*. The dorsoventral heights of the myosepta and longitudinal lengths of the myomeres were found to be negatively correlated in all three experiments. The time-series traces of myoseptum height and myomere length were found to be out of phase indicating a negative relationship between the two variables (Fig. 6a). This relationship was quantified using a reduced major axis linear regression (orthogonal regression), assuming equal variance for both variables. Prior to the regression analysis, the raw distance measurements were divided by the resting distance between the crystals, thereby converting them to normalized distances. Rest

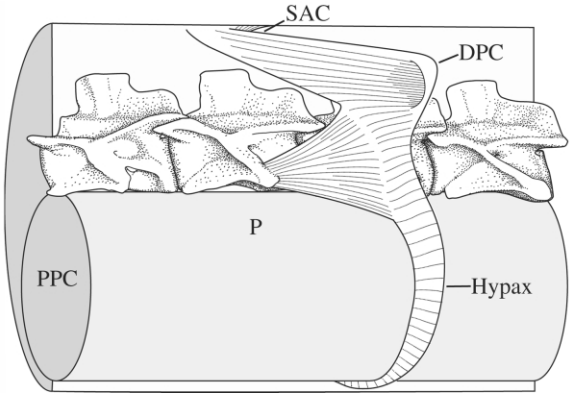

Fig. 5. Three-dimensional shape and collagen fiber orientation of trunk myosepta in *Siren lacertina*. *Abbreviations:* DPC, dorsal posterior cone; Hypax, hypaxial region of myoseptum; P, peritoneum; PPC, pleuroperitoneal cavity; SAC, secondary anterior cone.

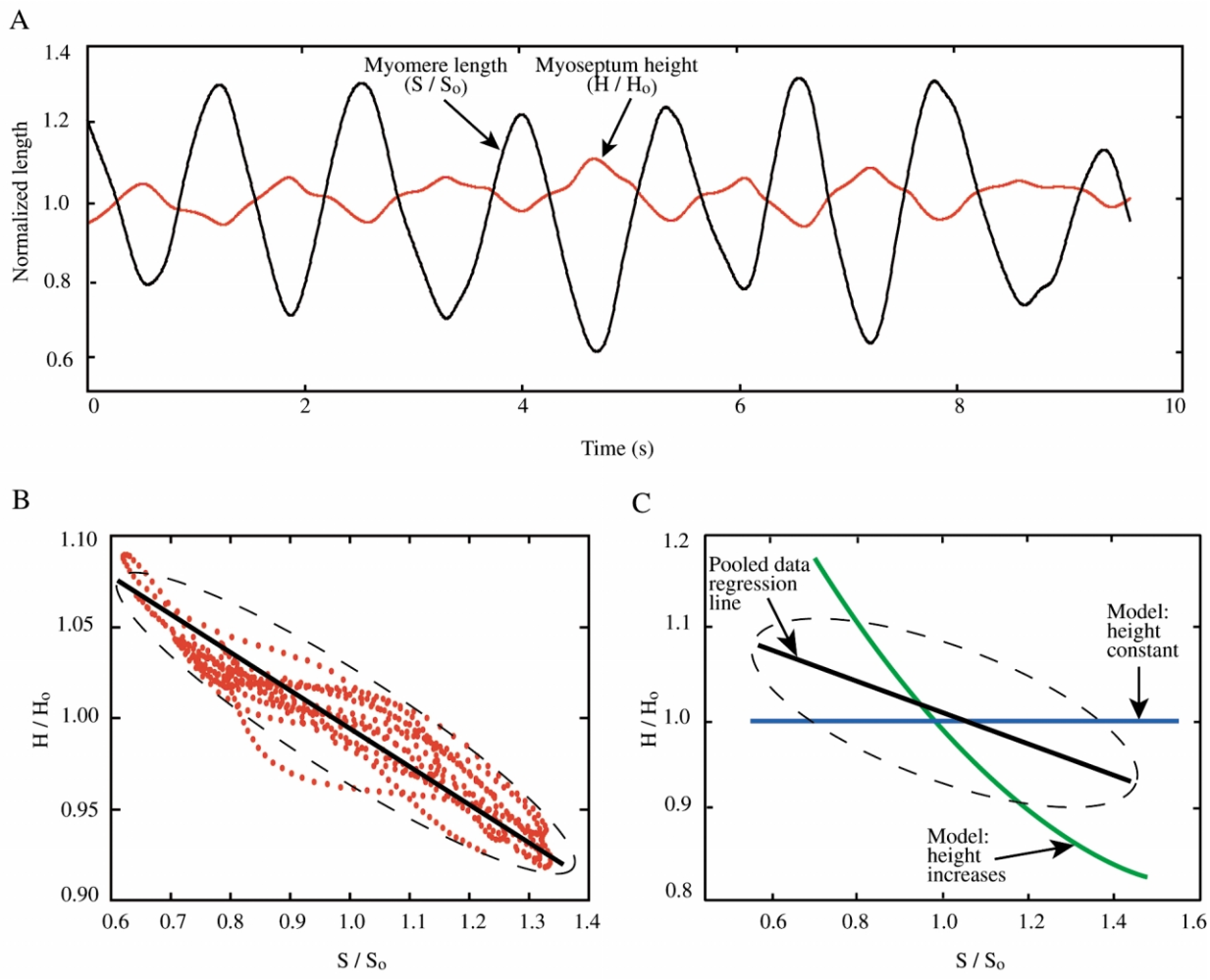

Fig. 6. Relationship between longitudinal length (S) of a myomere and dorsoventral height (H) of an adjacent myoseptum during steady swimming. (A) Sonomicrometry traces of a representative swimming sequence showing the normalized length of a myomere (black trace) and height of a myoseptum (red trace) vs. time. (B) Scatter plot of the normalized height of the myoseptum (H/H_o) vs. the normalized length of the myomere (S/S_o) for the same swimming sequence shown in (A). The data are fitted with a 95% density ellipse and a RMA regression line described by the equation $y=-0.18x+1.17$. The correlation coefficient (Pearson product-moment) for this swimming sequence is -0.937. (C) The 95% density ellipse and RMA regression line ($y=-0.19x+1.21$) for 25 swimming sequences (black). The correlation coefficient (Pearson product-moment) for the pooled data is -0.727. The empirically derived regression line (black) is shown alongside two predicted lines (green and blue) from the mathematical model. The blue line represents a model in which height of the myosepta remains constant during myomere shortening and the green line represents a model in which the height of the myosepta increases (see Figs. 2 and 3).

distances were determined when the animal was resting quietly on the bottom of the aquarium in a straight body position. The normalized data allowed for an easier comparison between the empirical relationship found here and the predicted values from the mathematical model.

In the first experiment (25 swimming sequences) the slopes for the reduced major axis (RMA) regressions of the normalized heights of myosepta (dorsoventral) vs. the normalized lengths of the myomere (longitudinal) ranged from -0.25 to -0.13 (Fig. 6b). For all 25 swimming sequences, the regression slopes were significantly different from zero. In order to compute a generalized relationship between the two normalized distances, data were pooled from all 25 swimming sequences and a RMA regression was performed. The pooled normalized myosepta heights and the pooled normalized myomere lengths have a negative linear correlation described by the equation $y=-0.19x+$

1.20 (Fig. 6c, black line). The 95% confidence interval for the slope of this regression is ± 0.005 and the Pearson product–moment correlation coefficient for this regression is -0.727 ($P=0.0001$).

In the second experiment (15 swimming sequences), the slopes for the RMA regressions of the normalized heights of myosepta vs. the normalized lengths of the myomere ranged from -0.51 to -0.16. For all 15 swimming sequences, the regression slopes were significantly different from zero. Data from all 15 swimming sequences were then pooled and a RMA regression was performed. The pooled normalized myosepta heights and the pooled normalized myomere lengths have a negative linear correlation described by the equation $y=-0.25x+1.30$. The 95% confidence interval for the slope of this regression is ± 0.005 and the Pearson product-moment correlation coefficient for this regression is -0.653 ($P=0.0001$).

In the third experiment, 10 startle response sequences were analyzed using a RMA regression of the normalized heights the myosepta vs. the normalized lengths of the myomere. The slopes of these regressions ranged from -0.40 to -0.18, and all 10 sequences had slopes that were significantly different from zero. For data pooled from all 10 escape sequences, we found that the normalized lengths of the myosepta and the normalized lengths of the myomere have a negative linear correlation described by the equation $y=-0.29x+1.29$. The 95% confidence interval for the slope of this regression is ± 0.006 and the Pearson product-moment correlation coefficient for this regression is -0.775 ($P=0.0001$).

The deformation of the myosepta recorded by sonomicrometry may be compared with the three conditions of myomere deformation explored in the mathematical model (Figs. 2 and 3). Sonomicrometry indicates that the dorsoventral height of the myosepta increases during segment shortening (Fig. 6), so clearly a model in which myomere height decreases (Fig. 2a) is not appropriate. During both steady swimming and startle responses, the dorsoventral deformation of the hypaxial myosepta is greater than predicted by the constant height model (Fig. 6c, blue line) but less than predicted by the height increases model (Fig. 6c, green line). For example, if a myomere were to shorten by 30%, the height increases model (Fig. 2c and Fig. 6c, green line) would predict a 19.5% increase in the dorsoventral height and a 19.5% increase in the mediolateral width of the myomere. However, based on the empirically derived regression line for our first swimming experiment (Fig. 6c, black line), the same 30% shortening of the myomere produces only a 6.7% increase in the dorsoventral height of myomere.

Combined with the high muscle fiber angle of the external oblique layer in *S. lacertina* (Fig. 1), the observed dorsoventral lengthening results in substantial amplification of muscle fiber shortening and segment shortening velocity. The external oblique in *S. lacertina* has a resting fiber angle of approximately 45° (Simons and Brainerd, 1999). We can plug this resting fiber angle (α) and our empirical measurements of the final length fraction of the segment (m) and changes in height (H) into the model to calculate the final length fraction of the muscle fibers (f), the strain amplification and the final muscle fiber angle (β). For a typical amount of myomere shortening observed during steady swimming (individual #1) ($m=0.7$ or 30% myomere shortening; Fig. 6b), we calculate that the final muscle fiber angle of the external oblique was 56° and the muscle fibers shortened 10.5% for a strain amplification of 2.87. This means that, for example, a muscle fiber shortening velocity of 10.0% s^{-1} would be amplified to a myomere shortening velocity of 28.7% s^{-1}. Similar results are obtained when data from the other two experiments are plugged back into our model. We calculate strain amplifications of 2.89 for the second (individual #2) steady swimming experiment and 3.12 for the startle response experiment.

4. Discussion

4.1. Interaction between muscle fiber angle and mechanics of myosepta

Previous studies of segmented musculature have focused either on muscle fiber architecture, de-emphasizing the role of myosepta and other axial connective tissues (Alexander, 1969), or on the morphology and mechanics of connective tissues, de-emphasizing the muscle fiber architecture within the myomeres (Wainwright et al., 1978; Westneat et al., 1993; Long et al., 1996; Westneat et al., 1998, but see Van Leeuwen, 1999 for an integrated approach). These previous studies have been concerned primarily with the axial morphology of fishes, in which both the three-dimensional shape of the segments and the muscle fiber trajec-

tories within the myomeres are highly complex. In contrast, the hypaxial myomeres of salamanders are relatively simple; muscle fiber angle is constant within each layer, the layers are nearly planar and the myosepta run in a roughly straight line from mid-lateral to ventral (Fig. 1). By studying the structure and function of both muscle fibers and connective tissues of an elongate salamander, *Siren lacertina*, we have developed a more integrated understanding of segmented muscle function.

We discovered that muscle fiber angle and myoseptal mechanics interact to determine the magnitude and velocity of myomere shortening. When myomeres shorten, they must expand (bulge) in the two dimensions orthogonal to shortening (to maintain constant volume, Alexander, 1969; Kier and Smith 1985). The direction of this bulging has a substantial impact on the way that muscle fiber shortening is converted to overall myomere shortening. In *S. lacertina*, if the myosepta and other axial connective tissues allow bulging in the dorsoventral direction, then the magnitude and speed of muscle fiber shortening will be greatly amplified (i.e. segment strain will be greater than muscle fiber strain). This strain amplification increases with increasing muscle fiber angle and increases with the ability of the myomeres to bulge in the dorsoventral direction (Figs. 2 and 3).

The mediolateral orientation of collagen fibers in the hypaxial myosepta of *S. lacertina* (Figs. 4 and 5) suggests that these myosepta are designed to allow dorsoventral bulging of the segment to occur. Sonomicrometry indicates that hypaxial myomeres do in fact bulge dorsoventrally during low amplitude steady swimming and during high amplitude startle responses in *S. lacertina* (Fig. 6). However, the observed dorsoventral bulging of the segment is less than that predicted by a model of an isolated muscle block, indicating that the myosepta or other axial connective tissues (such as skin) are limiting dorsoventral bulging to some extent. The hypaxial myomeres, therefore, benefit from some amplification of muscle fiber shortening, but not as much as predicted for an isolated muscle block (actual effect is intermediate between Fig. 3c and Fig. 3d).

Our finding that the myomeres bulge less in the dorsoventral direction than is predicted by a conservation of volume model means that they must be bulging more in the mediolateral direction. External observations of *S. lacertina* suggest that this mediolateral bulging occurs primarily in the region between the costal grooves. During axial bending, the concave side of a bent *S. lacertina* has a highly corrugated appearance with tissue bulging out between the costal grooves. This external appearance suggests that the myosepta are resisting mediolateral deformation, as expected from the mediolateral orientation of their collagen fibers, and that the volume of the muscle is conserved by mediolateral bulging between the myosepta. The myosepta resist mediolateral bulging of the myomere to the extent that they are able, thereby redirecting bulging into the dorsoventral direction and increasing the strain amplification of the muscle fibers. Further sonomicrometry will be necessary to quantify the mediolateral deformation of myosepta and myomeric bulging between the costal grooves.

4.2. Functions of myosepta

Previous workers have suggested that the two main functions of fish myosepta during locomotion are to transmit forces from the axial musculature to the vertebral column and to enhance force transmission by using intramuscular pressure to place axial connective tissues into tension (summarized in Westneat et al., 1998). To these we add the possibility that myosepta may increase the strain amplification of angled muscle fibers by controlling the way that myomeres bulge during contraction ('bulge control hypothesis').

If the primary function of the hypaxial myosepta in *S. lacertina* were to transmit forces through the anteromedially oriented attachment to the vertebral column (Fig. 5), then we would predict that the collagen fibers should have a dorsoventral orientation, or perhaps a combination of dorsoventral and mediolateral orientations. Instead, the orientation of collagen fibers in the hypaxial myomeres of *S. lacertina* is strongly mediolateral. This collagen fiber orientation suggests that a primary function of the myosepta is to resist mediolateral bulging and to allow dorsoventral bulging. Sonomicrometry results indicate that although some dorsoventral bulging does occur, the myomeres still bulge more in the mediolateral direction, presumably between the myosepta. However, if collagen fibers were oriented dorsoventrally, even less dorsoventral bulging would occur.

Our bulge control hypothesis is closely related to ideas about intramuscular pressure in fishes

(Wainwright et al., 1978; Westneat et al., 1993; McHenry et al., 1995; Long et al., 1996; Westneat et al., 1998). An isolated block of contracting muscle will bulge equally in the two dimensions orthogonal to shortening. With no limiting connective tissues, and no curved muscle fibers, this block of muscle will generate little or no intramuscular pressure (Otten, 1988). If, however, connective tissues limit bulging in one direction, then muscle pressure will increase and force extra bulging in the orthogonal direction. Previous studies have found that intramuscular pressure does indeed increase in swimming fishes (Wainwright et al., 1978; Westneat et al., 1998). Some of this increase in muscle pressure may be related to bulge control and muscle fiber strain amplification. The presence of intramuscular pressure satisfies a necessary condition of our model, but the generation of intramuscular pressure in fishes is highly complex and is almost certainly related to many different functions, such as the modulation of body stiffness (Long and Nipper, 1996) and the preloading of force transmission tissues (Wainwright et al., 1978; Westneat et al., 1998).

In contrast to hypaxial myosepta, the design of epaxial myosepta in *S. lacertina* is more clearly related to the transmission of muscular forces to the vertebral column (Fig. 5). Previous studies have shown that the epaxial regions of myomeres are active during steady swimming in salamanders (Frolich and Biewener, 1992; D'aout et al., 1996). In fish, transmission of such muscular forces in segmented musculature can occur through the direct attachment of myosepta to the vertebral column or through attachment to intermediate structures such as the horizontal septum, lamellae, skin, or a variety of axial tendons (Westneat et al., 1993; Gemballa and Britz, 1998; Vogel and Gemballa, 2000; Gemballa and Treiber, 2001; Hagen et al., 2001). In the epaxial myosepta of *S. lacertina*, the collagen fiber orientation is primarily longitudinal, indicating significant resistance to tension in the direction of axial bending (Fig. 5). In addition, the epaxial myosepta are directly attached to the vertebral column. At the boundary of the hypaxial and epaxial regions, an anteromedially-oriented region attaches each individual myoseptum to the transverse processes of vertebrae (Fig. 5). The fiber orientation and spatial arrangement of epaxial myosepta in *S. lacertina* suggest a substantial role in force transmission for epaxial myosepta.

In the abdominal region of vertebrates with segmented axial musculature, the shapes of the epaxial and hypaxial myomeres are markedly different from each other (Fig. 5 and Jayne and Lauder, 1994). This asymmetry is related to the presence of the abdominal cavity, and the epaxial and hypaxial myomeres become more similar in the caudal region (Jayne and Lauder, 1994). In *S. lacertina*, the different collagen fiber orientations within the abdominal myosepta may be related to the strong asymmetry in myomere shape between the epaxial and hypaxial regions. In the hypaxial region, the myosepta seem to be primarily designed to direct muscle bulging toward the dorsoventral direction, but they also certainly function to transmit hypaxial muscle force (and perhaps dorsoventral bulging is limited by the need for force transmission). In the epaxial region, the myosepta seem to be primarily designed to transmit muscle forces, but they may also be acting to control bulging. Modeling of epaxial myomeres combined with in vivo measurements of myomere shape change will be necessary to determine whether bulging is substantially modified by the more complex geometry of the epaxial region. A study of the morphology and function of abdominal myomeres in fishes may reveal a similar pattern of dorsoventral asymmetry and provide a useful system for examining the locomotory function of myosepta in fishes.

Acknowledgments

We thank Adam Summers and Tom Koob for inviting us to participate in the tendon symposium. We thank Sven Gemballa for helpful discussions, comments on the manuscript and for sharing with us an unpublished manuscript. We thank Alan Richmond for providing us with juvenile specimens of *Siren lacertina*. Will Sillen prepared Fig. 3 and Fig. 5. This material is based upon work supported by the US National Science Foundation under Grant No. 9875245 and the symposium was supported by NSF grant No. 0127260.

References

Alexander, R.Mc.N., 1969. The orientation of muscle fibers in the myomeres of fishes. J. Mar. Biol. Ass. UK 49, 263–290.

Bennett, W.O. III, Simons, R.S., Brainerd, E.L., 2001. Twisting and bending: the functional role of salamander lateral hypaxial musculature during locomotion. J. Exp. Biol. 200, 1979–1989.

Brainerd, E.L., Simons, R.S., 2000. Morphology and function of the lateral hypaxial musculature in salamanders. Am. Zool. 40, 77–86.

Carrier, D.R., 1993. Action of the hypaxial muscles during walking and swimming in the salamander *Dicamptodon ensatus*. J. Exp. Biol. 180, 75–83.

D'aout, K., Aerts, P., De Vrees, F., 1996. The timing of muscle strain and activation during steady swimming in a salamander *Ambystoma mexicanum*. Neth. J. Zool. 46, 263–271.

Ebmeyer, L., Gemballa, S., 2001. Locomotory system of *Ambystoma mexicanum*: anatomy and functional implications. J. Morphol. 248, 226.

Frolich, L.M., Biewener, A.A., 1992. Kinematic and electromyographic analysis of the functional role of the body axis during terrestrial and aquatic locomotion in the salamander, *Ambystoma tigrinum*. J. Exp. Biol. 162, 107–130.

Gans, C., 1989. Stages in the origin of vertebrates: analysis by means of scenarios. Biol. Rev. 64, 221–268.

Gemballa, S., Britz, R., 1998. Homology of intermuscular bones in acanthomorph fishes. Am. Mus. Novit. 3241, 1–25.

Gemballa, S., Treiber, K., 2001. Myosepta architecture of a cruising specialist and an accelerator: Are different modes of locomotion in *Scomber* and *Channa* driven by differently structured myosepta? J. Morphol. 248, 234.

Gillis, G.B., 1997. Anguilliform locomotion in an elongate salamander (*Siren intermedia*): effects of speed on axial undulatory movements. J. Exp. Biol. 200, 767–784.

Gillis, G.B., Biewener, A.A., 2000. Hindlimb extensor muscle function during jumping and swimming in the toad (*Bufo marinus*). J. Exp. Biol. 203, 3547–3563.

Greene, C.W., Greene, C.H., 1913. The skeletal musculature of the king salmon. Bull. Bur. Fish Wash. 33, 25–59.

Hagen, K., Gemballa, S., Freiwald, A., 2001. Locomotory design and locomotory habits of *Chimaera monstrosa*. J. Morphol. 248, 237.

Jayne, B.C., Lauder, G.V., 1994. Comparative morphology of the myomeres and axial skeleton in four genera of centrarchid fishes. J. Morphol. 220, 185–205.

Jayne, B.C., Lauder, G.V., 1995. Are muscle fibers within each myotome activated synchronously? Patterns of recruitment within deep myomeric musculature during swimming in largemouth bass. J. Exp. Biol. 198, 805–815.

Kier, W.M., Smith, K.K., 1985. Tongues, tentacles and trunks: the biomechanics of movements in hydrostats. Zool. J. Linn. Soc. 83, 307–324.

Long, J.H., Nipper, K.S., 1996. The importance of body stiffness in undulatory propulsion. Am. Zool. 36, 678–694.

Long, J.H., Hale, M.E., McHenry, M.J., Westneat, M.W., 1996. Functions of fish skin: the mechanics of steady swimming in longnose gar *Lepisosteus osseus*. J. Exp. Biol. 199, 2139–2151.

Maurer, F., 1911. Die ventrale Rumpfmuskulatur von *Menobranchus*, *Menopoma* und *Amphiuma*. Jena. Zeits. Naturwiss. 47, 1–42.

Maurer, F., 1913. Die ventrale Rumpfmuskulatur der Fische (Selachier, Ganoiden, Teleostier, Crossopterygier, Dipnoer). Jena. Zeitschr. Naturwiss. 49, 1–118.

McHenry, M.J., Pell, C.A., Long, J.H., 1995. Mechanical control of swimming speed: stiffness and axial wave form in undulating fish models. J. Exp. Biol. 198, 2293–2305.

Otten, E., 1988. Concepts and models of functional architecture in skeletal muscle. Exercise Sports Sci. Rev. 16, 89–137.

Rome, L.C., Swank, D., Corda, D., 1993. How fish power swimming. Science 261, 340–343.

Shadwick, R.E., Katz, S.L., Korsmeyer, K.E., Knower, T., Covell, J.W., 1999. Muscle dynamics in skipjack tuna: timing of red muscle shortening in relation to activation and body curvature during steady swimming. J. Exp. Biol. 202, 2139–2150.

Shann, E.W., 1914. On the nature of the lateral muscle in Teleostei. Proc. Zool. Soc. Lond. 1914, 319–337.

Simons, R.S., Brainerd, E.L., 1999. Morphological variation of the hypaxial musculature in salamanders. J. Morphol. 241, 153–164.

Van Leeuwen, J.L., 1999. A mechanical analysis of myomere shape in fish. J. Exp. Biol. 2002, 3405–3414.

Vogel, F., Gemballa, S., 2000. Locomotory design of cyclostome fishes: spatial arrangement and architecture of myosepta and lamellae. Acta Zool. 81, 267–283.

Wainwright, S.A., 1983. To bend a fish. In: Webb, P.W., Weihs, D. (Eds.), Fish Biomechanics. Praeger Press, New York, pp. 68–91.

Wainwright, S.A., Vosburgh, F., Hebrank, J.H., 1978. Shark skin: function in locomotion. Science 202, 747–749.

Wakeling, J.M., Johnston, I.A., 1999. White muscle strain in the common carp and red to white muscle gearing ratios in fish. J. Exp. Biol. 202, 521–528.

Westneat, M.W., Hoese, W., Pell, C.A., Wainwright, S.A., 1993. The horizontal septum: mechanics of force transfer in locomotion of scombrid fishes (Scombridae, Perciformes). J. Morphol. 217, 183–204.

Westneat, M.W., Hale, M.E., McHenry, M.J., Long, J.H., 1998. Mechanics of the fast-start: muscle function and the role of intramuscular pressure in the escape behavior of *Amia calva* and *Polypterus palmas*. J. Exp. Biol. 201, 3041–3055.

Willemse, J.J., 1966. The functional anatomy of the myosepta of fishes. Proc. K. Ned. Akad. Wet., Ser. A Math. Sci. 69, 58–63.